Quantitative MHC class-I/-II expression levels in *CDK12* mutated prostate cancer patients reveal intratumorally T cell adaptive immune response in tumors

William Lautert-Dutra[1]; Camila M. Melo[1]; Luiz Paulo Chaves[1]; Rodolfo Borges dos Reis[1]; Jeremy A. Squire[1,2]

[1] Department of Genetics, Medicine School of Ribeirão Preto, University of São Paulo, Ribeirão Preto 14048-900, SP, Brazil; [2] Division of Urology, Department of Surgery and Anatomy, Medicine School of Ribeirão Preto, University of São Paulo, Ribeirão Preto 14048-900, SP, Brazil; [3] Department of Pathology and Molecular Medicine, Queen's University, Kingston, ON K7L3N6, Canada.

Abstract

Treatment of advanced prostate cancer (PCa) remains a therapeutic challenge. The promising improvements provided by new immune-checkpoint blockade (ICB) therapies have shown only modest benefits in a minority of PCa patients. *CDK12* defective-PCa is a recently described immune active class of advanced PCa with an elevated mutational burden, high inflammatory levels, and increased immune cell infiltrate. *CDK12* has been proposed as a predictive biomarker of treatment response to ICB since partial response treatment has been found among *CDK12* PCa patients treated with ICB. This study was designed to investigate potential molecular causes of alterations to immune response among patient tumors with defects of *CDK12* in primary (TCGA-PRAD, n = 48) and metastatic (mCRPC-SU2C, n = 10) PCa. We hypothesize that the expression of the MHC-I and -II genes would differ in the *CDK12* defective tumors, which would explain the lack of response in some patients treated with ICB. Using RNA-seq data, we were able to distinguish two groups of tumors with *CDK12* defective tumors based on differential MHC expression. Tumors with increased MHC levels showed the activation of several pathways associated with the immune system and elevated *PD-L1*, *IDO1*, and *TIM3* expression. There was also increased composition of CD8+ T cells, B cells, γδ T cells, and M1 Macrophages in tumors with elevated MHC levels. These data suggest that MHC expression and associated immune response pathways may provide new biomarkers for ICB therapeutic response in *CDK12*-defective PCa.

Introduction

Treatment of advanced prostate cancer (PCa) remains a therapeutic challenge. The life expectancy of diagnosed patients largely depends on the tumor grade and an early diagnosis.

Men with distant metastases at diagnosis have the worst overall survival (OS), with only 30% of patients surviving > 5 years (Rebello et al., 2021). For recurrent disease, acquired resistance to Androgen Deprivation Therapy (ADT) and chemotherapy remains a significant cause of death (Wong et al., 2016). While immune-checkpoint blockade (ICB) therapies, such as PD-L1 inhibition, have shown significant benefits in only a minority of patients (Binnewies et al., 2018). Thus, it is necessary to discover and characterize the genetic pathways and molecular signatures that could help to predict the best treatments for advanced PCa.

The tumor mutation burden affects the infiltration of immune cells in the TME, which sets tumors with impaired DNA damage repair (DDR) as a target for immune therapies (Schumacher & Schreiber, 2015). The biallelic inactivation of Cyclin-dependent Kinase 12, *CDK12*, was recently described as a novel immune active class of advanced PCa with a high mutation burden, an inflammatory phenotype and immune cell infiltrate distinct from other defective molecular subtypes (Nguyen et al., 2020; Rescigno et al., 2021; Sokol et al., 2019; Y. M. Wu et al., 2018). In a retrospective multi-center study, Antonarakis *et al.* found that *CDK12*-altered advanced PCa is a more aggressive subtype with poor outcomes to first-line therapy (Antonarakis et al., 2020). In the same work, nine men received PD-1 inhibition therapy (pembrolizumab and nivolumab); 33% of the patients had a prostate-specific antigen (PSA) response and increased progression-free survival of 5.4 months. Additionally, Schweizer *et al.* investigate the differences between standard treatments and ICB in *CDK12* metastatic castration-resistant prostate cancer (mCRPC) (Schweizer et al., 2020). In this study, nineteen mCRPC received ICB; eleven out of nineteen (59%) of the patients had a decline in PSA, with two patients (11%) having a 100% PSA decline. Therefore, despite having *CDK12* alterations, some patients from this molecular subgroup were non-responsive to ICB treatment, and the causes of this resistance were poorly understood.

Tumor cells may develop various types of escape mechanisms that allow them to avoid recognition and destruction by the immune system. For example, the expression of checkpoint proteins (PD-1/PD-L1, CTLA-4, LAG3) (Spranger & Gajewski, 2018) by tumors may increase pro-tumorigenic immune cell infiltration (Tregs, M2 Macrophages) (Horton et al., 2019). Tumors may also develop intrinsic cancer-cell signaling that can suppress the activity of infiltrating immune cells (WNT/β-catenin) (Li et al., 2019). Another mechanism exploited by tumors to avoid the recognition of cytotoxic T cells (CD8+) and antigen-presenting cells (APCs) is through loss of major histocompatibility complex class-I or class-II (MHC-I and MHC-II) (McGranahan et al., 2017).

The loss of MHC-I and MHC-II may occur reversibly or irreversibly, and change has been linked to tumor progression, poor prognosis, and reduced response to ICB in different malignancies (Dhatchinamoorthy et al., 2021; Thibodeau et al., 2012). As classified by Garrido et al., the alteration in the MHC expression is divided into two major groups: "Soft" alterations, those capable of recovering or upregulating MHC antigens after cytokine exposure (e.g., regulatory abnormalities); "Hard" alterations, those that cannot recover MHC expression (e.g., structural defects) (Garrido & Aptsiauri, 2019). During tumor evolution, the infiltration of cytotoxic lymphocytes eliminates highly immunogenic tumor clones causing a selection of surviving cell populations that have acquired MHC alterations (Algarra et al., 2021). The low expression of MHC-I in colorectal cancer has been associated with a poor prognosis (Watson et al., 2006). In melanoma patients, loss of expression of MHC-I and MHC-II was associated with resistance to anti-CTLA-4, and anti-PD-1, respectively (Rodig et al., 2018). The enhanced response to ICB in melanoma and Hodgkin lymphoma is thought to be due to the expression of MHC-II and PD-L1 in both tumors (Johnson et al., 2018; Roemer et al., 2018). In PCa there is presently limited information on the role of MHC-I and MHC-II expression and ICB response.

In prostate cancer, *CDK12* inactivation is known to increase the immunogenicity of tumor cells but the relationship between *CDK12* loss and MHC expression has not been investigated. Changes in expression of MHC-I and -II are known to be involved in tumor immune evasion in various types of cancer. There is also evidence that anti-cancer T cell immune activity contributes to the selection of tumor cells with lower levels of MHC expression. However, the molecular mechanisms responsible for reducing MHC expression are poorly understood. Hence, we hypothesize that the expression of the MHC-I and -II genes would differ in the *CDK12* defective tumors and could provide predictive information on pathways mediating ICB response. Thus, the implementation of a combined measure between *CDK12* mutation and the presence of MHC expression may better predict outcomes for prostate cancer tumors classified as eligible for ICB treatment based on *CDK12*-subtype and normal antigen presentation function.

Material and Methods

Cohort

We used The CbioPortal for Cancer Genomics (Gao et al., 2013) to search primary (pPCa) and metastatic (mCRPC) prostate tumor cohorts, including *CDK12* defective samples,

101 and to download clinical information from patients. The classification of samples having
102 *CDK12* loss-of-function followed previous reports and was based on the Onco Query Language
103 pattern (OQL) (CDK12: MUT, CDK12: HETLOSS, CDK12: HOMDEL, CDK12: AMP)
104 (Nguyen et al., 2020; Rescigno et al., 2021; Sokol et al., 2019). Only cohorts containing *CDK12*
105 altered-RNA-seq samples data were selected in the Genotypes and Phenotypes (dbGaP) data-
106 base and applied for access under project ID 29255 (**Figure S1**, **Table-S1**).
107
108 ***RNA-Seq data analysis***
109 For the pPCa, we used the package recount2 to download summarized experiments
110 objects containing the transcription-level RNA-Seq abundance matrix from the TCGA-Prostate
111 Adenocarcinoma (TCGA-PRAD) (Abeshouse et al., 2015; Imada et al., 2019). Additionally,
112 for the mCRPC, we download SRA Paired-End (PE) reads using the SRAToolkit
113 (https://github.com/ncbi/sra-tools). The quality of the raw reads was then measured using the
114 FASTQC program (https://www.bioinformatics.babraham.ac.uk/projects/fastqc/). We quanti-
115 fied the expression of transcripts using the software Salmon v1.6.0 (Patro et al., 2017) in the
116 human transcriptome. The transcriptome index was built using the reference GRCh38 version
117 of the human genome (http://ftp.ensembl.org/pub/release-105/fasta/homo_sapi-
118 ens/dna/Homo_sapiens.GRCh38.dna.primary_assembly.fa.gz) and transcriptome
119 (https://ftp.ebi.ac.uk/pub/databases/gencode/Gencode_human/release_39/gencode.v39.tran-
120 scripts.fa.gz), downloaded from ENSEMBL and GENCODE, following the instruction man-
121 ual. We used then used the Tximport v1.22.0 package to import the transcription-level abun-
122 dance and estimate raw counts derived from the quantification step (Soneson et al., 2015). The
123 count data normalization, expression levels, and differential gene expression (DEG) analysis
124 for both pPCa and mCRPC cohorts were executed using the DESeq2 v1.34.0 (Love et al., 2014;
125 Zhu et al., 2019). We used the clusterProfiler v4.2.1 and enrichR (https://maayanlab.cloud/En-
126 richr/) to implement equally over-representation (ORA) enrichment analysis and gene set en-
127 richment analysis (GSEA) of the DEGs and the whole transcriptome profile, respectively, us-
128 ing the Gene Ontology (GO) and Molecular Signatures Database (MSigDB) (Carbon et al.,
129 2019; Khatri et al., 2012; Liberzon et al., 2015; Subramanian et al., 2005; T. Wu et al., 2021)
130 (**Figure S1**).
131
132 ***MHC expression***
133 We performed hierarchical clustering analysis using a representative subset of MHC
134 genes (Schaafsma et al., 2021), and we observed two groups of *CDK12* defective tumors

regarding MHC expression as shown in Figure S2. We used an arbitrary cutoff of quartile to divide the *CDK12* defective tumors into "High" and "Low" expressed MHC-I and -II groups (Koopman et al., 2000). For the quartile quantification, we used the normalized expression values of the classical genes that composed each MHC class (e.g., MHC-I, *HLA-A*, *HLA-B*, *HLA-C*; MHC-II, *HLA-DPA1*, *HLA-DPB1*, *HLA-DQA1*, *HLA-DQA1*, *HLA-DQB1*, *HLA-DQB2*, *HLA-DRA*, *HLA-DQB1*, *HLA-DRB5*, *HLA-DRB6*) (Schaafsma et al., 2021). We dichotomized expression levels to be below or above the first quartile for each gene, we then used this classification to generate the final logical values regarding the patient's MHC status ('High' or 'Low' expressed) (**Fig. S2**). Samples were classified as having MHC 'Low' expression when at least one gene composing each class was expressed at a low level. In mCRPC *CDK12*- defective, all tumors classified as MHC-High presented similar high expression of both MHC-I and -II (henceforth, mCRPC *CDK12* defective MHC High), thus we called these tumors just MHC High. The summary values used to classify the tumors are shown in table S2. The final logical values for the pPCa and mCRPC are shown in S3, S4, S5, and S6.

Digital cytometry

To investigate and quantify the immune cell composition in the TME of tumors having *CDK12* defects, we used the bulk tissue gene expression profiles (GEP) from RNA-seq data from both pPCa and mCRPC with the digital cytometry CIBERSORTx (https://cibersortx.stanford.edu) (Chen et al., 2018; Newman et al., 2015). Briefly, this program uses bulk tissue GEP, compares the data with prior knowledge of expression profiles from purified leukocytes, and estimates a relative immune abundance composition in the tumor. We used the 'signature matrix' containing a validated leukocyte GEP of 22 human hematopoietic cell phenotypes, LM22, to estimate the immune cell composition from the TME (**Fig. S1**).

Computational and statistical analysis

We used a GNU/Linux environment to perform the quality control and quantify the raw reads to the human transcriptome. Subsequently, the processed data was used in the downstream analysis in RStudio software (R Foundation for Statistical Computing, R v4.1.2), and all results were plotted either by ViDGER v1.14.0 or ggplot2 (McDermaid et al., 2019; Wickham et al., 2016) (Fig. S1). Pearson Correlation was used to perform a correlation analysis of the normalized expression levels (coef. level = 0.95). A gene was considered differentially expressed when log2 foldchange > 1 expressed from the reference group with a *p*-adjusted value < 0.05. For the enrichment analysis, we used a cutoff value of 0.05.

Results

Transcriptomics

Since immune evasion by cancer cells is associated with altered MHC, we expected that the expression of the MHC-I and -II genes would differ among the *CDK12* defective tumors. It follows that downstream altered pathways could provide predictive information on poor ICB responses in this molecular subtype of prostate cancer. To investigate MHC expression levels in PCa further, we compared the transcriptomics of *CDK12* defective (*CDK12* defective) prostate tumors classified as "MHC High" (top 75% quartile) to the transcriptomics of *CDK12* deficient tumors classified as having a low expression of MHC genes (bottom 25% quartile).

CDK12 defective MHC-I/-II High-expression tumors showed distinct transcriptome profiles with upregulation of IFN-γ-responsive genes and an inflamed TME

We first compared the transcriptome of *CDK12* defective PCa classified as MHC-High and compared to *CDK12* defective tumors MHC-Low groups in pPCa and mCRPC (Figure S2, Figure 1A-B,). The pPCa *CDK12* defective MHC-I High showed 1319 upregulated and 2153 downregulated genes (**Table-S7, Table-S8**). Three clusters of gene expression were apparent in our comparison (**Figure 1A**). The upper cluster (I) has *IGHV* and *IGLV* over-expressed genes linked to *CDK12* MHC I high. The middle cluster (II) has four HLA genes overexpressed in the MHC I high group, which supports our classification based on *CDK12* defective MHC expression and upregulation of many genes related to antigen presentation and CD8+ T cell activity (e.g., *HLA-A*, *HLA-B*, *HLA-C*, *B2M*, *GZMB*, *PSMB9, LCK, SOCS1*) (**Figure 1B**). The lower cluster (III) has 14 downregulated genes when MHC I is highly expressed. Likewise, *CDK12* defective MHC-II High exhibited 1129 upregulated and 580 downregulated genes (**Table-S7, Table-S9)**. Two clusters were apparent in our comparison (**Figure 1B**). The upper cluster showed the upregulation of genes related to cytotoxicity, immune cell migration, and immune suppression (e.g., *GZMA*, *IL12RB1*, *CD27*, *CD48*, *PRF1*, *CD8A*, *TNFRSF9*, *VCAM1*, *IL32*, *CD22*, *CD74,* and *TIGIT*) (**Figure 1B**). Second, the mCRPC *CDK12* defective MHC-High 230 upregulated and 46 downregulated genes (**Table-S7, Table-S10)**. The combined MHC I and II showed two distinct clusters (**Figure 1C**). The lower cluster showed the upregulation of genes linked to innate and adaptative immune response and CD4+ and CD8+ T cell activity (e.g., *DEFA1*, *CD79B*, *CD3* (*e*, *d*, *g*), *TRBC2*, *KLRK1*, *CD27*, *NKG7*, *IL18RAP*, *IL2RG*, *BLK*, *CD5*, *CD8* (*a*, *b*), *IL12RB1*, *ICOS*, *PRF1*, *CD96*, *CD247*) (**Figure 1C**). In

203 conclusion, for both pPCa and mCRPC, *CDK12* defective MHC high gene expression is asso-
204 ciated with transcriptomic changes that are indicative of a general pattern of activation of IFN-
205 γ-responsive and cytotoxic activity genes. The next step was to perform enrichment analysis to
206 identify potential functional associations of expression changes associated with *CDK12* defec-
207 tive MHC High/Low clusters.

208 To better understand the transcriptional alterations in *CDK12* defective tumors classi-
209 fied as MHC-I/-II high-expressed, we used ORA and GSEA analysis to investigate the func-
210 tional activity of the gene expression changes of both cohorts. In pPCa, patient tumors with
211 *CDK12* defective MHC-I high-expressed showed activation of interferon-γ-response, activa-
212 tion of immune cells, and antigen presentation by MHC-I pathways (**Figure 1D**, **Table-S8**). In
213 pPCa with *CDK12* defective MHC-II high-expressed also showed high pathways activity of
214 antigen presentation through MHC-II, as expected (**Figure 1E, Table-S9**). Next, mCRPC
215 *CDK12* defective MHC high-expressed exhibited activation of cytotoxicity and adaptative cy-
216 totoxicity immune response (**Figure 1F, Table-S10**). Furthermore, GSEA analysis showed ac-
217 tivation of many Hallmarks pathways in *CDK12* defective MHC-I high-expressed (e.g., Epi-
218 thelial-Mesenchymal Transition, Inflammatory Response, Interferon Gamma Response, Inter-
219 feron Alpha Response, TNFA Signaling via NFKB, P53, and IL2/STAT5 Signaling (**Figure**
220 **3A, Table-S8**). In addition, the *CDK12* defective MHC-II High group had similar pathway
221 activation, but with the addition of Allograft Rejection (**Figure 3B, Table-S9**). Likewise,
222 mCRPC *CDK12* defective MHC high showed activation of various Hallmarks and Reactome
223 pathways (e.g., Allograft Rejection, Interferon Gamma Response, Inflammatory Response, In-
224 terferon Alpha Response, IL2/STAT5 Signaling, Apoptosis, TCR Signaling, Interleukin 10
225 Signaling, Constitutive Signaling by Aberrant PI3K in Cancer, and the suppressive PD1 Sig-
226 naling pathway (**Figure 3C-D, Table-S10**). Collectively, our transcriptomic analysis suggests
227 that *CDK12* defective PCa with high MHC expression displays the activation of various path-
228 ways associated with the immune system.

229

230 ***CDK12 defective MHC-I/-II High groups exhibited tumor microenvironment with high ex-***
231 ***pression of chemokines and immunomodulatory genes in both cohorts***.

232 To elucidate the underlying immunologic signature in TME of *CDK12* defective MHC
233 high expression groups, we investigate the difference between chemokines and immunomod-
234 ulatory genes expression between conditions. In pPCa, the *CDK12* defective MHC-I High ex-
235 hibited upregulation of many chemokines linked to APCs and effector T cell migration (e.g.,
236 *CCL2*, *CCL7*, *CCL19*, *CCL21*, *CXCL1, CXCL2, CXCL5, CXCL8, CXCL10, CXCL12,*

237 *CXCL13*, *CXCL16, CX3CL1*) (**Figure S3)** and the immunomodulatory genes *HAVCR2* (*TIM3*)
238 and *IDO1*. (**Figure 2A-B**). Also, *CDK12* defective MHC-II High presented increased expres-
239 sion of chemokines related to Natural killer, T effector cell, and B cell infiltration (e.g., *CCL8*,
240 *CCL19*, *CCL22*, *CXCL13*) (**Figure S3**), and the immunomodulatory genes *CD274* (*PD-L1*),
241 *HAVCR2* (*TIM3*), and *IDO1* (**Figure 2C-E**). Based on Pearson Correlation analysis, we ob-
242 served a significant positive correlation within MHC-I complex genes and with *IDO1* but with
243 no other investigated gene (**Figure S6A**). Interestingly, among the MHC-II genes, correlation
244 analysis showed a significant positive association between the expression of the MHC-II com-
245 plex and the immunomodulatory genes, *CD274* (*PD-L1*), *IDO1*, and *HAVCR2*(*TIM3*) (**Figure**
246 **S6B**). In mCRPC with *CDK12* defective MHC high-expressed, we detected a high expression
247 of chemokines *CCL4*, *CCL5, CXCL9*, *CXCL12* (**Figure S4**), and the immunomodulatory gene
248 *CD274* (*PD-L1*) (**Figure 2F**). Furthermore, we observed a significant positive association be-
249 tween the immunomodulatory genes *HAVCR2*(*TIM3*) and *CTLA4*, *LAG3*, and the expression
250 of MHC-I and -II genes (**Figure S6C-D**). As shown, MHC high-expression *CDK12* defective
251 tumors had a pattern of high chemokine expression and upregulation of inhibitory mechanisms.
252
253 ***Immune cell composition***
254 Our transcriptomics analysis predicts that *CDK12* defective MHC-I/-II High expressing
255 tumors will display enrichment of immune cells with high effector and cytotoxic activity, and
256 the co-inhibitory expression of inhibitory pathways by tumor cells. To test this hypothesis, we
257 used *in silico* cytometry (CIBERSORTx, https://cibersortx.stanford.edu) algorithm to estimate
258 the immune cell composition in the TME of pPCa and mCRPC CDK12 defective with MHC
259 high-expressed.
260
261 ***CDK12 defective MHC-I/-II High CDK12 loss-of-function tumors showed distinct immune***
262 ***cell infiltrate in the TME.***
263 We investigated whether MHC-I and -II high expression would affect the variation in
264 immune cell composition in *CDK12* defective tumors in both cohorts. We found that *CDK12*
265 defective MHC high-expressed tumors displayed ongoing increased APCs and effector lym-
266 phocytes traffic in their TME **(Figure 4**). In pPCa, *CDK12* defective MHC-I high-expressed
267 pPCa showed a significant increase in the composition of Naïve B cells, CD8+ T cells, and γδ
268 T cells, while the reduced composition of Mastocytes (**Figure 4A**). In comparison, the *CDK12*
269 defective MHC-II high-expressed exhibited an increase of γδ T cells and reduced composition
270 of Plasma cells and M0 macrophages (**Figure 4B**). Additionally, in mCRPC, *CDK12*-Mut

MHC high-expressed showed a significative increased composition of CD8+ T cell and M1 Macrophages. (**Figure 4C**).

Discussion

In prostate cancer, *CDK12* inactivation is known to increase the immunogenicity of tumor cells (Lotan & Antonarakis, 2021). Changes in MHC-I and -II expression are involved in tumor immune evasion in various types of cancer. Using RNA-seq data, we observed two groups of *CDK12* defective tumors regarding MHC expression. MHC high-expressed groups showed the activation of various pathways associated with the immune system and significantly high *PD-L1*, *IDO1*, and *TIM3* expression and increased CD8+ T cells, B cells, γδ T cells, and M1 composition Macrophages in *CDK12* defective classified as MHC High.

Our clinical analysis showed that MHC-I High and MHC High in pPCa and mCRPC, respectively, exhibited a trend towards better overall survival when compared to the MHC lower expression group ($p > 0.05$, **Figure S7**). Several studies have similarly found that the expression of the MHC-I and -II genes are associated with better clinical outcomes and different resistance mechanisms (Park et al., 2017; Rodig et al., 2018; Roemer et al., 2018). Rodig *et al*. showed that the lack of MHC-I expression in melanoma was linked to higher odds of progressive disease and resistance to anti-CTLA4, but not to anti-PD1. In the same study, expression of MHC-II in tumors was associated with tumors that were more likely to respond to anti-PD1 ICB treatment. In Hodgkin Lymphoma treated with nivolumab (anti-PD1), analysis of malignant Hodgkin Reed-Sternberg cells showed MHC-II expression, but not MHC-I, was predictive of complete remission and longer PFS in (Roemer et al., 2018). Park et al. showed that MHC-II positivity in tumor cells was associated with better disease-free survival in patients with lymph node metastasis (Park et al., 2017). From a practical standpoint, these results suggest that analysis of MHC-I and -II expression levels could be used to determine whether *CDK12* defective prostate cancer tumors are more likely to respond to ICB treatments. Further study of downstream MHC-dependent immunomodulatory signals may also provide insights into other pathways leading to immunotherapy failure.

Transcriptomic signatures associated with MHC expression variation have been described in different tumor types and they appear to capture the activity of genes and biological pathways related to clinical responses to ICB (Ayers et al., 2017; Johnson et al., 2016, 2018; Rodig et al., 2018; Schaafsma et al., 2021). Ayers *et al.* proposed a gene expression profile with the composition of eighteen genes relevant to predicting the clinical outcome of anti-PD1.

304 This IFN-γ gene signature in pretreatment tumor biopsies was associated with better outcomes
305 in melanoma, head-and-neck squamous cell carcinoma, and gastric cancer treated with pem-
306 brolizumab (Ayers et al., 2017). In our study, the *CDK12* patient tumors classified as MHC
307 High showed the presence of several genes previously described as IFN-γ-responsive and cy-
308 totoxic activity and associated with response to anti-PD1 therapy (**Figure S8**). Our results also
309 showed the activation of pathways related to IFN-γ response and production in both the pPCA
310 and mCRPC cohorts (**Figure 1 B, D, F**). Gene Set Enrichment Analysis showed that *CDK12*
311 defective tumors demonstrate signatures of "Allograft rejection" and "IL2_STAT5 signaling"
312 (**Figure 3 B, D, Figure 4 B-C**). Interestingly, only the mCRPC *CDK12* MHC High showed
313 the signature of "PD-1 signaling", but pPCa *CDK12* MHC-II and mCRPC *CDK12* MHC High
314 showed significantly higher expression of *CD274* (*PD-L1*) (**Figure 2**). These results suggest
315 that the intrinsic inflammatory signal from *CDK12* defective tumors classified as 'MHC High'
316 may potentiate these tumor cells to upregulate the expression of MHC-I and MHC-II and pre-
317 sent endogenous peptides to CD8+ and CD4+ T Helper cells, matching higher *PD-L1* expres-
318 sion on tumor cells (Younger et al., 2008).

319 Alternative immunomodulatory mechanisms promote adaptative resistance to thera-
320 peutic anti-PD1(Koyama et al., 2016). We identified the upregulation of immunomodulatory
321 molecules, such as *IDO1* and *TIM3* in both MHC-I and -II *CDK12* defective pPCa (**Figure 2**).
322 Also, in pPCa, we found a positive correlation of MHC-I genes with IDO1 and MHC-II genes
323 with *PDCD1* (*PD-1*), *CD274* (*PD-L1*), *LAG3*, *IDO1*, and *HAVCR2*(*TIM3*) (**Figure S6 A-B**).
324 In mCRPC, we found a positive correlation of MHC-I and -II genes expression with
325 *HAVCR2*(*TIM3*) and *CTLA4*, *LAG3* (**Figure S6 C-D**). Our findings may indicate the presence
326 of an acquired resistance mechanism in a subset of *CDK12* defective prostate cancer tumors
327 classified as MHC High (i.e., upregulation of immunomodulatory molecules). These results
328 suggest that the measure of the basal expression of MHC genes could be developed as a bi-
329 omarker to characterize *CDK12* patient samples with a previously inflamed environment and
330 the expression of immunomodulatory genes linked to resistance to anti-PD1 (i.e., upregulation
331 of *IDO1* and *TIM3*)

332 The expression of MHC molecules plays a pivotal role in providing the signals neces-
333 sary to recognize and activate the immune system against tumor neoantigens and is essential
334 to controlling tumor growth through cytotoxic activity (Qin et al., 2005; Schreiber et al., 2011).
335 We found a higher abundance of CD8+ T cells in both *CDK12* defective pPCa MHC-I and
336 mCRPC MHC. Interestingly, only in the CDK12 pPCa were we able to find increased levels
337 of γδ T cells. This result may either indicate the dependence of CD8+ T cells in MHC-I antigen

presentation or suggest that enhanced CD4+ Th infiltrate could support the continued accumulation of CD8+ CTLs in the tumor microenvironment (Johnson et al., 2016). Also, the basal effector immune cell population such as γδ T cells, in pPCa, may be responsible, in part, for IFN-γ, and may indicate the dependence of the MHC-unrestricted recognition role of γδ T cells and its presence in the TME (Born et al., 2006; Rodig et al., 2018).

Interestingly, we found a link between *IGHV* and *IGLV* over-expressed genes to *CDK12* defective pPCa MHC-I high-expressed (upper cluster I, **Figure 1A**). The production of Ig by tumors cells (cancer-derived Ig) is described in a variety of tumors, as well as in prostate cancer (Cui et al., 2021; Li et al., 2011; Pan et al., 2013; C. Qin et al., 2020). Also, cancer-derived Ig may act as checkpoint proteins and inhibit the function of effector T cells and NK cells (Li et al., 2011; Wang et al., 2020). Therefore, the upregulation of cancer-specific Ig may reflect a parallel immune escape mechanism in *CDK12* MHC-I high-expressed in response to MHC-I/CD8+ T cell antigen recognition.

Importantly, this study did not address the molecular mechanism underlying the alteration of MHC genes expression in *CDK12* defective prostate cancer samples. The loss of MHC expression could be derived from two different mechanisms of disruption (Garrido et al., 2010). First, regulatory abnormalities downregulate the expression of MHC genes through mechanisms that do not affect the genomic structure of HLA genes, and the MHC expression can be recovered by specific T-cell mediated response (e.g., IFN-γ signaling). Second, during tumor evolution, the infiltration of cytotoxic lymphocytes eliminates tumor clones high immunogenic causing a selection of clones that may present structural alteration, or "Hard" lesions, in the MHC loci or other genomic regions (e.g., *B2M*, *IFN*, *STAT*) distinct from the derived clone (Zaretsky et al., 2016). After selection, these clones will be invisible to the immune system and the lesion will progress (Algarra et al., 2021). However, further studies approaching the causes of MHC disruption and how altered expression in *CDK12* defective prostate cancer are needed. Furthermore, because the non-tumor cell content was not defined in this study, we were unable to establish a limit for the contribution of the *CDK12* defective tumor cells since the RNA-seq relies on data from bulk tissue, and the DEGs analysis of a varying mixture of immune and tumor cells may not give precise results (van den Berge et al., 2019).

Using RNA-seq data, we observed two groups of *CDK12* defective tumors based on variation in MHC expression levels. Our data suggest that *CDK12* defective MHC high-expressing PCa would have an active and inflamed tumor microenvironment with elevated immunomodulatory pathway expression and increased presence of effector T cells. More extensive *in vitro* and *in vivo* investigations are required to relate this molecular subtype to potential

actionable immunomodulatory mechanisms or possible therapeutic targets in PCa. These findings also provide support for investigations into the clinical use of MHC expression levels in *CDK12* defective prostate cancer to identify tumors likely to respond to ICB treatment.

Bibliography

Abeshouse, A., Ahn, J., Akbani, R., Ally, A., Amin, S., Andry, C. D., Annala, M., Aprikian, A., Armenia, J., Arora, A., Auman, J. T., Balasundaram, M., Balu, S., Barbieri, C. E., Bauer, T., Benz, C. C., Bergeron, A., Beroukhim, R., Berrios, M., … Zmuda, E. (2015). The Molecular Taxonomy of Primary Prostate Cancer. *Cell*, *163*(4), 1011–1025. https://doi.org/10.1016/j.cell.2015.10.025

Algarra, I., Garrido, F., & Garcia-Lora, A. M. (2021). MHC heterogeneity and response of metastases to immunotherapy. In *Cancer and Metastasis Reviews* (Vol. 40, Issue 2, pp. 501–517). Springer. https://doi.org/10.1007/s10555-021-09964-4

Antonarakis, E. S., Pedro, ;, Velho, I., Fu, W., Wang, H., Agarwal, N., Victor, ;, Santos, S., Maughan, B. L., Pili, R., Adra, N., Sternberg, C. N., Panagiotis, ;, Vlachostergios, J., Tagawa, S. T., Bryce, A. H., Mcnatty, A. L., Reichert, Z. R., Dreicer, R., … Hussain, M. (2020). CDK12-Altered Prostate Cancer: Clinical Features and Therapeutic Outcomes to Standard Systemic Therapies, Poly (ADP-Ribose) Polymerase Inhibitors, and PD-1 Inhibitors. In *JCO Precis Oncol* (Vol. 4). https://doi.org/10.

Ayers, M., Lunceford, J., Nebozhyn, M., Murphy, E., Loboda, A., Kaufman, D. R., Albright, A., Cheng, J. D., Kang, S. P., Shankaran, V., Piha-Paul, S. A., Yearley, J., Seiwert, T. Y., Ribas, A., & McClanahan, T. K. (2017). IFN-γ-related mRNA profile predicts clinical response to PD-1 blockade. *Journal of Clinical Investigation*, *127*(8), 2930–2940. https://doi.org/10.1172/JCI91190

Binnewies, M., Roberts, E. W., Kersten, K., Chan, V., Fearon, D. F., Merad, M., Coussens, L. M., Gabrilovich, D. I., Ostrand-Rosenberg, S., Hedrick, C. C., Vonderheide, R. H., Pittet, M. J., Jain, R. K., Zou, W., Howcroft, T. K., Woodhouse, E. C., Weinberg, R. A., & Krummel, M. F. (2018). Understanding the tumor immune microenvironment (TIME) for effective therapy. *Nature Medicine*, *24*(5), 541–550. https://doi.org/10.1038/s41591-018-0014-x

Born, W. K., Reardon, C. L., & O'Brien, R. L. (2006). The function of γδ T cells in innate immunity. In *Current Opinion in Immunology* (Vol. 18, Issue 1, pp. 31–38). https://doi.org/10.1016/j.coi.2005.11.007

Carbon, S., Douglass, E., Dunn, N., Good, B., Harris, N. L., Lewis, S. E., Mungall, C. J., Basu, S., Chisholm, R. L., Dodson, R. J., Hartline, E., Fey, P., Thomas, P. D., Albou, L. P., Ebert, D., Kesling, M. J., Mi, H., Muruganujan, A., Huang, X., … Westerfield, M. (2019). The Gene Ontology Resource: 20 years and still GOing strong. *Nucleic Acids Research*, *47*(D1), D330–D338. https://doi.org/10.1093/nar/gky1055

Chen, B., Khodadoust, M. S., Liu, C. L., Newman, A. M., & Alizadeh, A. A. (2018). Profiling tumor infiltrating immune cells with CIBERSORT. In *Methods in Molecular Biology* (Vol. 1711, pp. 243–259). Humana Press Inc. https://doi.org/10.1007/978-1-4939-7493-1_12

414 Cui, M., Huang, J., Zhang, S., Liu, Q., Liao, Q., & Qiu, X. (2021). Immunoglobulin Expres-
415 sion in Cancer Cells and Its Critical Roles in Tumorigenesis. *Frontiers in Immunol-*
416 *ogy*, *12*. https://doi.org/10.3389/fimmu.2021.613530
417 Dhatchinamoorthy, K., Colbert, J. D., & Rock, K. L. (2021). Cancer Immune Evasion
418 Through Loss of MHC Class I Antigen Presentation. *Frontiers in Immunology*, *12*.
419 https://doi.org/10.3389/fimmu.2021.636568
420 Gao, J., Aksoy, B. A., Dogrusoz, U., Dresdner, G., Gross, B., Sumer, S. O., Sun, Y., Jacob-
421 sen, A., Sinha, R., Larsson, E., Cerami, E., Sander, C., & Schultz, N. (2013). Integra-
422 tive analysis of complex cancer genomics and clinical profiles using the cBioPortal.
423 *Science Signaling*, *6*(269). https://doi.org/10.1126/scisignal.2004088
424 Garrido, F., & Aptsiauri, N. (2019). Cancer immune escape: MHC expression in primary
425 tumours versus metastases. In *Immunology* (Vol. 158, Issue 4, pp. 255–266). Black-
426 well Publishing Ltd. https://doi.org/10.1111/imm.13114
427 Garrido, F., Cabrera, T., & Aptsiauri, N. (2010). "Hard" and "soft" lesions underlying the
428 HLA class I alterations in cancer cells: Implications for immunotherapy. In *Interna-*
429 *tional Journal of Cancer* (Vol. 127, Issue 2, pp. 249–256).
430 https://doi.org/10.1002/ijc.25270
431 Horton, B. L., Fessenden, T. B., & Spranger, S. (2019). Tissue Site and the Cancer Im-
432 munity Cycle. In *Trends in Cancer* (Vol. 5, Issue 10, pp. 593–603). Cell Press.
433 https://doi.org/10.1016/j.trecan.2019.07.006
434 Imada, E. L., Sanchez, D. F., Collado-Torres, L., Wilks, C., Matam, T., Dinalankara, W.,
435 Stupnikov, A., Lobo-Pereira, F., Yip, C. W., Yasuzawa, K., Kondo, N., Itoh, M., Su-
436 zuki, H., Kasukawa, T., Hon, C. C., de Hoon, M. J. L., Shin, J. W., Carninci, P., Jaffe,
437 A. E., … Marchionni, L. (2019). Recounting the FANTOM Cage Associated Transcrip-
438 tome. *BioRxiv*. https://doi.org/10.1101/659490
439 Johnson, D. B., Bordeaux, J., Kim, J. Y., Vaupel, C., Rimm, D. L., Ho, T. H., Joseph, R. W.,
440 Daud, A. I., Conry, R. M., Gaughan, E. M., Hernandez-Aya, L. F., Dimou, A.,
441 Funchain, P., Smithy, J., Witte, J. S., McKee, S. B., Ko, J., Wrangle, J. M., Dabbas, B.,
442 … Dakappagari, N. (2018). Quantitative spatial profiling of PD-1/PD-L1 interaction
443 and HLA-DR/IDO-1 predicts improved outcomes of anti-PD-1 therapies in meta-
444 static melanoma. *Clinical Cancer Research*, *24*(21), 5250–5260.
445 https://doi.org/10.1158/1078-0432.CCR-18-0309
446 Johnson, D. B., Estrada, M. v., Salgado, R., Sanchez, V., Doxie, D. B., Opalenik, S. R.,
447 Vilgelm, A. E., Feld, E., Johnson, A. S., Greenplate, A. R., Sanders, M. E., Lovly, C.
448 M., Frederick, D. T., Kelley, M. C., Richmond, A., Irish, J. M., Shyr, Y., Sullivan, R. J.,
449 Puzanov, I., … Balko, J. M. (2016). Melanoma-specific MHC-II expression repre-
450 sents a tumour-autonomous phenotype and predicts response to anti-PD-1/PD-L1
451 therapy. *Nature Communications*, *7*. https://doi.org/10.1038/ncomms10582
452 Khatri, P., Sirota, M., & Butte, A. J. (2012). Ten years of pathway analysis: Current ap-
453 proaches and outstanding challenges. In *PLoS Computational Biology* (Vol. 8, Issue
454 2). https://doi.org/10.1371/journal.pcbi.1002375
455 Koopman, L. A., Corver, W. E., van der Slik, A. R., Giphart, M. J., & Fleuren, G. J. (2000).
456 Multiple Genetic Alterations Cause Frequent and Heterogeneous Human Histo-
457 compatibility Leukocyte Antigen Class I Loss in Cervical Cancer. *Journal of Experi-*
458 *mental Medicine*, *191*(6), 961–976. https://doi.org/10.1084/jem.191.6.961
459 Koyama, S., Akbay, E. A., Li, Y. Y., Herter-Sprie, G. S., Buczkowski, K. A., Richards, W. G.,
460 Gandhi, L., Redig, A. J., Rodig, S. J., Asahina, H., Jones, R. E., Kulkarni, M. M.,

Kuraguchi, M., Palakurthi, S., Fecci, P. E., Johnson, B. E., Janne, P. A., Engelman, J. A., Gangadharan, S. P., … Hammerman, P. S. (2016). Adaptive resistance to therapeutic PD-1 blockade is associated with upregulation of alternative immune checkpoints. *Nature Communications*, *7*. https://doi.org/10.1038/ncomms10501

Li, X., Ni, R., Chen, J., Liu, Z., Xiao, M., Jiang, F., & Lu, C. (2011). The Presence of IGHG1 in Human Pancreatic Carcinomas Is Associated With Immune Evasion Mechanisms. *Pancreas*, *40*(5), 753–761. https://doi.org/10.1097/MPA.0b013e318213d51b

Li, X., Xiang, Y., Li, F., Yin, C., Li, B., & Ke, X. (2019). WNT/β-catenin signaling pathway regulating T cell-inflammation in the tumor microenvironment. In *Frontiers in Immunology* (Vol. 10, Issue SEP). Frontiers Media S.A. https://doi.org/10.3389/fimmu.2019.02293

Liberzon, A., Birger, C., Thorvaldsdóttir, H., Ghandi, M., Mesirov, J. P., & Tamayo, P. (2015). The Molecular Signatures Database Hallmark Gene Set Collection. *Cell Systems*, *1*(6), 417–425. https://doi.org/10.1016/j.cels.2015.12.004

Lotan, T. L., & Antonarakis, E. S. (2021). CDK12 deficiency and the immune microenvironment in prostate cancer. *Clinical Cancer Research*, *27*(2), 380–382. https://doi.org/10.1158/1078-0432.CCR-20-3877

Love, M. I., Huber, W., & Anders, S. (2014). Moderated estimation of fold change and dispersion for RNA-seq data with DESeq2. *Genome Biology*, *15*(12). https://doi.org/10.1186/s13059-014-0550-8

McDermaid, A., Monier, B., Zhao, J., Liu, B., & Ma, Q. (2019). Interpretation of differential gene expression results of RNA-seq data: Review and integration. In *Briefings in Bioinformatics* (Vol. 20, Issue 6, pp. 2044–2054). Oxford University Press. https://doi.org/10.1093/bib/bby067

McGranahan, N., Rosenthal, R., Hiley, C. T., Rowan, A. J., Watkins, T. B. K., Wilson, G. A., Birkbak, N. J., Veeriah, S., van Loo, P., Herrero, J., Swanton, C., Jamal-Hanjani, M., Shafi, S., Czyzewska-Khan, J., Johnson, D., Laycock, J., Bosshard-Carter, L., Gorman, P., Hynds, R. E., … Dessimoz, C. (2017). Allele-Specific HLA Loss and Immune Escape in Lung Cancer Evolution. *Cell*, *171*(6), 1259-1271.e11. https://doi.org/10.1016/j.cell.2017.10.001

Newman, A. M., Liu, C. L., Green, M. R., Gentles, A. J., Feng, W., Xu, Y., Hoang, C. D., Diehn, M., & Alizadeh, A. A. (2015). Robust enumeration of cell subsets from tissue expression profiles. *Nature Methods*, *12*(5), 453–457. https://doi.org/10.1038/nmeth.3337

Nguyen, B., Mota, J. M., Nandakumar, S., Stopsack, K. H., Weg, E., Rathkopf, D., Morris, M. J., Scher, H. I., Kantoff, P. W., Gopalan, A., Zamarin, D., Solit, D. B., Schultz, N., & Abida, W. (2020). Pan-cancer Analysis of CDK12 Alterations Identifies a Subset of Prostate Cancers with Distinct Genomic and Clinical Characteristics. *European Urology*, *78*(5), 671–679. https://doi.org/10.1016/j.eururo.2020.03.024

Pan, B., Zheng, S., Liu, C., & Xu, Y. (2013). Suppression of IGHG1 gene expression by siRNA leads to growth inhibition and apoptosis induction in human prostate cancer cell. *Molecular Biology Reports*, *40*(1), 27–33. https://doi.org/10.1007/s11033-012-1944-x

Park, I. A., Hwang, S.-H., Song, I. H., Heo, S.-H., Kim, Y.-A., Bang, W. S., Park, H. S., Lee, M., Gong, G., & Lee, H. J. (2017). Expression of the MHC class II in triple-negative breast cancer is associated with tumor-infiltrating lymphocytes and interferon

signaling. *PLOS ONE*, *12*(8), e0182786. https://doi.org/10.1371/journal.pone.0182786

Patro, R., Duggal, G., Love, M. I., Irizarry, R. A., & Kingsford, C. (2017). Salmon provides fast and bias-aware quantification of transcript expression. *Nature Methods*, *14*(4), 417–419. https://doi.org/10.1038/nmeth.4197

Qin, C., Sheng, Z., Huang, X., Tang, J., Liu, Y., Xu, T., & Qiu, X. (2020). Cancer-driven IgG promotes the development of prostate cancer though the SOX2-CIgG pathway. *The Prostate*, *80*(13), 1134–1144. https://doi.org/10.1002/pros.24042

Qin, H., Zhou, C., Wang, D., Ma, W., Liang, X., Lin, C., Zhang, Y., & Zhang, S. (2005). Specific antitumor immune response induced by a novel DNA vaccine composed of multiple CTL and T helper cell epitopes of prostate cancer associated antigens. *Immunology Letters*, *99*(1), 85–93. https://doi.org/10.1016/j.imlet.2005.01.006

Rebello, R. J., Oing, C., Knudsen, K. E., Loeb, S., Johnson, D. C., Reiter, R. E., Gillessen, S., van der Kwast, T., & Bristow, R. G. (2021). Prostate cancer. *Nature Reviews Disease Primers*, *7*(1). https://doi.org/10.1038/s41572-020-00243-0

Rescigno, P., Gurel, B., Pereira, R., Crespo, M., Rekowski, J., Rediti, M., Barrero, M., Mateo, J., Bianchini, D., Messina, C., Fenor de la Maza, M. D., Chandran, K., Carmichael, J., Guo, C., Paschalis, A., Sharp, A., Seed, G., Figueiredo, I., Lambros, M., … de Bono, J. S. (2021). Characterizing CDK12-mutated prostate cancers A C. *Clinical Cancer Research*, *27*(2), 566–574. https://doi.org/10.1158/1078-0432.CCR-20-2371

Rodig, S. J., Gusenleitner, D., Jackson, D. G., Gjini, E., Giobbie-Hurder, A., Jin, C., Chang, H., Lovitch, S. B., Horak, C., Weber, J. S., Weirather, J. L., Wolchok, J. D., Postow, M. A., Pavlick, A. C., Chesney, J., & Hodi, F. S. (2018). MHC proteins confer differential sensitivity to CTLA-4 and PD-1 blockade in untreated metastatic melanoma. In *Sci. Transl. Med* (Vol. 10). https://www.science.org

Roemer, M. G. M., Redd, R. A., Cader, Z., Pak, C. J., Abdelrahman, S., Ouyang, J., Sasse, S., Younes, A., Fanale, M., Santoro, A., Zinzani, P. L., Timmerman, J., Collins, G. P., Ramchandren, R., Cohen, J. B., de Boer, J. P., Kuruvilla, J., Savage, K. J., Trneny, M., … Shipp, M. A. (2018). *JOURNAL OF CLINICAL ONCOLOGY Major Histocompatibility Complex Class II and Programmed Death Ligand 1 Expression Predict Outcome After Programmed Death 1 Blockade in Classic Hodgkin Lymphoma*. https://doi.org/10.1200/JCO

Schaafsma, E., Fugle, C. M., Wang, X., & Cheng, C. (2021). Pan-cancer association of HLA gene expression with cancer prognosis and immunotherapy efficacy. *British Journal of Cancer*, *125*(3), 422–432. https://doi.org/10.1038/s41416-021-01400-2

Schreiber, R. D., Old, L. J., & Smyth, M. J. (n.d.). *Cancer Immunoediting: Integrating Immunity's Roles in Cancer Suppression and Promotion*. www.sciencemag.org

Schumacher, T. N., & Schreiber, R. D. (2015). Neoantigens in cancer immunotherapy. In *Science* (Vol. 348, Issue 6230, pp. 69–74). American Association for the Advancement of Science. https://doi.org/10.1126/science.aaa4971

Schweizer, M. T., Ha, G., Gulati, R., Brown, L. C., McKay, R. R., Dorff, T., Hoge, A. C. H., Reichel, J., Vats, P., Kilari, D., Patel, V., Oh, W. K., Chinnaiyan, A., Pritchard, C. C., Armstrong, A. J., Montgomery, R. B., & Alva, A. (2020). CDK12 -Mutated Prostate Cancer: Clinical Outcomes With Standard Therapies and Immune Checkpoint Blockade . *JCO Precision Oncology*, *4*, 382–392. https://doi.org/10.1200/po.19.00383

Sokol, E. S., Pavlick, D., Frampton, G. M., Ross, J. S., Miller, V. A., Ali, S. M., Lotan, T. L., Pardoll, D. M., Chung, J. H., & Antonarakis, E. S. (2019). Pan-Cancer Analysis of CDK12 Loss-of-Function Alterations and Their Association with the Focal Tandem-Duplicator Phenotype . *The Oncologist*, *24*(12), 1526–1533. https://doi.org/10.1634/theoncologist.2019-0214

Soneson, C., Love, M. I., & Robinson, M. D. (2015). Differential analyses for RNA-seq: transcript-level estimates improve gene-level inferences. *F1000Research*, *4*, 1521. https://doi.org/10.12688/f1000research.7563.1

Spranger, S., & Gajewski, T. F. (2018). Mechanisms of Tumor Cell-Intrinsic Immune Evasion. *Annu. Rev. Cancer Biol*, *2*, 213–228. https://doi.org/10.1146/annurev-cancerbio

Subramanian, A., Tamayo, P., Mootha, V. K., Mukherjee, S., Ebert, B. L., Gillette, M. A., Paulovich, A., Pomeroy, S. L., Golub, T. R., Lander, E. S., & Mesirov, J. P. (2005). *Gene set enrichment analysis: A knowledge-based approach for interpreting genome-wide expression profiles*. www.pnas.orgcgidoi10.1073pnas.0506580102

Thibodeau, J., Bourgeois-Daigneault, M.-C., & Lapointe, R. (2012). Targeting the MHC Class II antigen presentation pathway in cancer immunotherapy. *OncoImmunology*, *1*(6), 908–916. https://doi.org/10.4161/onci.21205

van den Berge, K., Hembach, K. M., Soneson, C., Tiberi, S., Clement, L., Love, M. I., Patro, R., & Robinson, M. D. (2019). RNA Sequencing Data: Hitchhiker's Guide to Expression Analysis. *Annual Review of Biomedical Data Science*, *2*(1), 139–173. https://doi.org/10.1146/annurev-biodatasci-072018-021255

Wang, Z., Geng, Z., Shao, W., Liu, E., Zhang, J., Tang, J., Wang, P., Sun, X., Xiao, L., Xu, W., Zhang, Y., Cui, H., Zhang, L., Yang, X., Chang, X., & Qiu, X. (2020). Cancer-derived sialylated IgG promotes tumor immune escape by binding to Siglecs on effector T cells. *Cellular & Molecular Immunology*, *17*(11), 1148–1162. https://doi.org/10.1038/s41423-019-0327-9

Watson, N. F. S., Ramage, J. M., Madjd, Z., Spendlove, I., Ellis, I. O., Scholefield, J. H., & Durrant, L. G. (2006). Immunosurveillance is active in colorectal cancer as downregulation but not complete loss of MHC class I expression correlates with a poor prognosis. *International Journal of Cancer*, *118*(1), 6–10. https://doi.org/10.1002/ijc.21303

Wickham, H., Chang, W., Henry, L., Pedersen, T. L., Takahashi, K., Wilke, C., & Woo, K. (2016). *ggplot2: Elegant Graphics for Data Analysis*. Springer-Verlag New York.

Wong, M. C. S., Goggins, W. B., Wang, H. H. X., Fung, F. D. H., Leung, C., Wong, S. Y. S., Ng, C. F., & Sung, J. J. Y. (2016). Global Incidence and Mortality for Prostate Cancer: Analysis of Temporal Patterns and Trends in 36 Countries. *European Urology*, *70*(5), 862–874. https://doi.org/10.1016/j.eururo.2016.05.043

Wu, T., Hu, E., Xu, S., Chen, M., Guo, P., Dai, Z., Feng, T., Zhou, L., Tang, W., Zhan, L., Fu, X., Liu, S., Bo, X., & Yu, G. (2021). clusterProfiler 4.0: A universal enrichment tool for interpreting omics data. *The Innovation*, *2*(3). https://doi.org/10.1016/j.xinn.2021.100141

Wu, Y. M., Cieślik, M., Lonigro, R. J., Vats, P., Reimers, M. A., Cao, X., Ning, Y., Wang, L., Kunju, L. P., de Sarkar, N., Heath, E. I., Chou, J., Feng, F. Y., Nelson, P. S., de Bono, J. S., Zou, W., Montgomery, B., Alva, A., Robinson, D. R., & Chinnaiyan, A. M. (2018). Inactivation of CDK12 Delineates a Distinct Immunogenic Class of

601 Advanced Prostate Cancer. *Cell*, *173*(7), 1770-1782.e14.
602 https://doi.org/10.1016/j.cell.2018.04.034
603 Younger, A. R., Amria, S., Jeffrey, W. A., Mahdy, A. E. M., Goldstein, O. G., Norris, J. S., &
604 Haque, A. (2008). HLA class II antigen presentation by prostate cancer cells. *Pros-*
605 *tate Cancer and Prostatic Diseases*, *11*(4), 334–341.
606 https://doi.org/10.1038/sj.pcan.4501021
607 Zaretsky, J. M., Garcia-Diaz, A., Shin, D. S., Escuin-Ordinas, H., Hugo, W., Hu-Lieskovan,
608 S., Torrejon, D. Y., Abril-Rodriguez, G., Sandoval, S., Barthly, L., Saco, J., Homet
609 Moreno, B., Mezzadra, R., Chmielowski, B., Ruchalski, K., Shintaku, I. P., Sanchez,
610 P. J., Puig-Saus, C., Cherry, G., … Ribas, A. (2016). Mutations Associated with Ac-
611 quired Resistance to PD-1 Blockade in Melanoma. *New England Journal of Medi-*
612 *cine*, *375*(9), 819–829. https://doi.org/10.1056/nejmoa1604958
613 Zhu, A., Ibrahim, J. G., & Love, M. I. (2019). Heavy-Tailed prior distributions for se-
614 quence count data: Removing the noise and preserving large differences. *Bioinfor-*
615 *matics*, *35*(12), 2084–2092. https://doi.org/10.1093/bioinformatics/bty895
616
617
618 **Figures Legends**
619
620
621 **Figure 1. MHC-I/-II high expression in CDK12 defective prostate cancer showed**
622 **distinct transcriptome activity. (A)** Transcriptome heatmap exhibiting clustering of top
623 50 DEGs in pPCa CDK12-Mut MHC-I High group (n = 30). The upper cluster (I) has
624 IGHV and IGLV over-expressed genes linked to *CDK12* MHC I high. The middle cluster
625 (II) has four HLA genes overexpressed in MHC I high group, which supports our classi-
626 fication based on *CDK12* mutated MHC expression. The lower cluster (III) has 14 down-
627 regulated genes when MHC I is highly expressed. **(B)** Transcriptome heatmap exhibiting
628 clustering of top 50 DEGs in the pPCa CDK12-Mut MHC-II High group (n = 23). The
629 upper cluster (I) has upregulation of genes related to cytotoxicity, immune cell migration,
630 and immune suppression. We could not observe clinical features associated with clusters
631 of either MHC I or II. **(C)** Transcriptome heatmap exhibiting clustering of top 50 DEGs
632 in the mCRPC CDK12-Mut MHC High group (n = 6). The combined MHC I and II
633 showed two distinct clusters. The lower cluster showed the upregulation of genes linked
634 to innate and adaptative immune response and CD4+ and CD8+ T cell activity **(D)** En-
635 riched GO (BP) pathways of the upregulated genes from pPCa CDK12-Mut MHC-I. **(E)**
636 Enriched GO (BP) pathways of the upregulated genes from pPCa CDK12-Mut MHC-II
637 High group. **(F)** Enriched GO (BP) pathways of the upregulated genes from the mCRPC
638 CDK12-Mut High group. The DEGs are relative to the CDK12-Mut 'Low' group. Clinical
639 information is displayed on top of the heatmap for each patient. The color scale in the
640 heatmap represents the Z-score of the normalized read counts for each gene, where the
641 red scale color indicates upregulated, and blue low expressed genes. Enrichment analyses
642 were performed using *clusterProfiler* and p-adjusted value = 0.05 as the cutoff. Bar plots
643 show the top 20 most significant Gene Ontology (BP) terms.
644
645 **Figure 2. MHC high expressed CDK12 defective prostate cancer showed enhanced**
646 **expression of immunomodulatory genes.** RNA-sequencing expression level of im-
647 munomodulatory genes **(A)** *IDO1* (p < 0.018), **(B)** *HAVCR2* (*TIM3*) (p < 0.0022) in
648 *CDK12-Mut* MHC-I High. n = 48; **(C)** *CD274* (*PD-L1*) (p < 0.0028), **(D)** *HAVCR2* (*TIM3*)
649 (p < 0.00012), **(E)** *IDO1* (p < 0.001) in *CDK12-Mut* MHC-II High. n = 48; **(F)** *CD274*

650 (*PD-L1*) ($p < 0.0095$). $n = 10$; *: p-value < 0.05; **: p-value < 0.01, by Mann-Whitney
651 test. *IDO1*, Indoleamine 2,3-Dioxygenase 1; *HAVCR3* (*TIM3*), T-Cell Immunoglobulin
652 Mucin Receptor 3; *CD274* (*PD-L1*), Programmed Cell Death 1 Ligand 1.
653 **Figure 3. MHC high expressed *CDK12* defective prostate tumors are associated with**
654 **activation of immune-related pathways. (A)** Gene Set Enrichment Analysis of Hall-
655 mark's pathways in pPCa *CDK12-Mut* MHC-I High ($n = 30$)**. (B)** Gene Set Enrichment
656 Analysis of Hallmark pathways in pPCa *CDK12-Mut* MHC-II High ($n = 23$). **(C-D)** Gene
657 Set Enrichment Analysis of Hallmarks and Reactome pathways in mCRPC *CDK12-Mut*
658 MHC High ($n = 10$). A normalized enrichment score indicates each factor's positive or
659 negative association with the condition of interest, which means activation or suppression
660 of the pathway. Enrichment analyses were performed using *clusterProfiler* and p-adjusted
661 value = 0.05 as the cutoff.
662
663 **Figure 4. MHC high expressed *CDK12* defective are associated with enhanced T cell**
664 **recruitment in primary and advanced prostate tumors. (A)** CIBERSORT-derived im-
665 mune cell abundance of 22 distinct cell subsets based on *CDK12* defective MHC-I High
666 pPCa ($n = 30$)**. (B)** CIBERSORT-derived immune cell abundance of 22 distinct cell sub-
667 sets based on *CDK12* defective MHC-II High pPCa ($n = 23$). **(C)** CIBERSORT-derived
668 immune cell abundance of 22 distinct cell subsets based on *CDK12* defective MHC High
669 mCRPC ($n = 10$). *: p-value < 0.05; **: p-value < 0.01, by Mann-Whitney test.
670

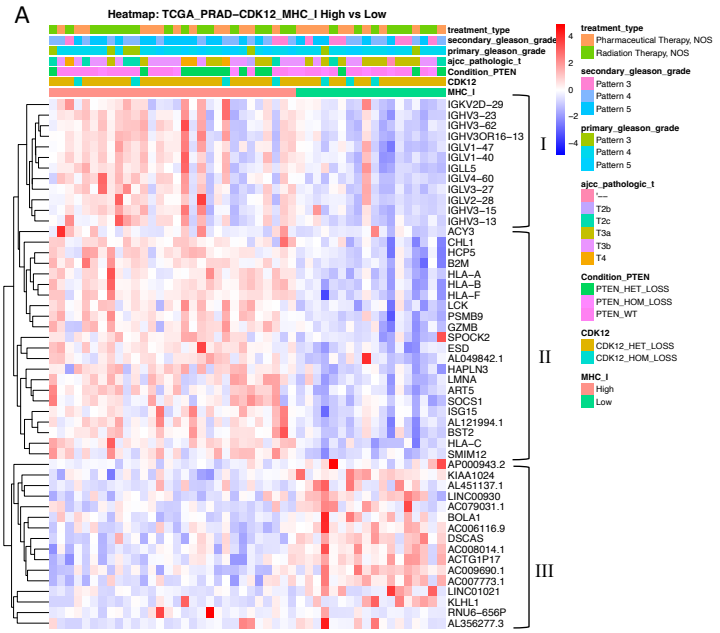
A
Heatmap: TCGA_PRAD–CDK12_MHC_I High vs Low
treatment_type
secondary_gleason_grade
primary_gleason_grade
ajcc_pathologic_t
Condition_PTEN
CDK12
MHC_I
IGKV2D–29
IGHV3–23
IGHV3–62
IGHV3OR16–13
IGLV1–47
IGLV1–40
IGLL5
IGLV4–60
IGLV3–27
IGLV2–28
IGHV3–15
IGHV3–13
ACY3
CHL1
HCP5
B2M
HLA–A
HLA–B
HLA–F
LCK
PSMB9
GZMB
SPOCK2
ESD
AL049842.1
HAPLN3
LMNA
ART5
SOCS1
ISG15
AL121994.1
BST2
HLA–C
SMIM12
AP000943.2
KIAA1024
AL451137.1
LINC00930
AC079031.1
BOLA1
AC006116.9
DSCAS
AC008014.1
ACTG1P17
AC009690.1
AC007773.1
LINC01021
KLHL1
RNU6–656P
AL356277.3
I
II
III
treatment_type
Pharmaceutical Therapy, NOS
Radiation Therapy, NOS
secondary_gleason_grade
Pattern 3
Pattern 4
Pattern 5
primary_gleason_grade
Pattern 3
Pattern 4
Pattern 5
ajcc_pathologic_t
'–––
T2b
T2c
T3a
T3b
T4
Condition_PTEN
PTEN_HET_LOSS
PTEN_HOM_LOSS
PTEN_WT
CDK12
CDK12_HET_LOSS
CDK12_HOM_LOSS
MHC_I
High
Low

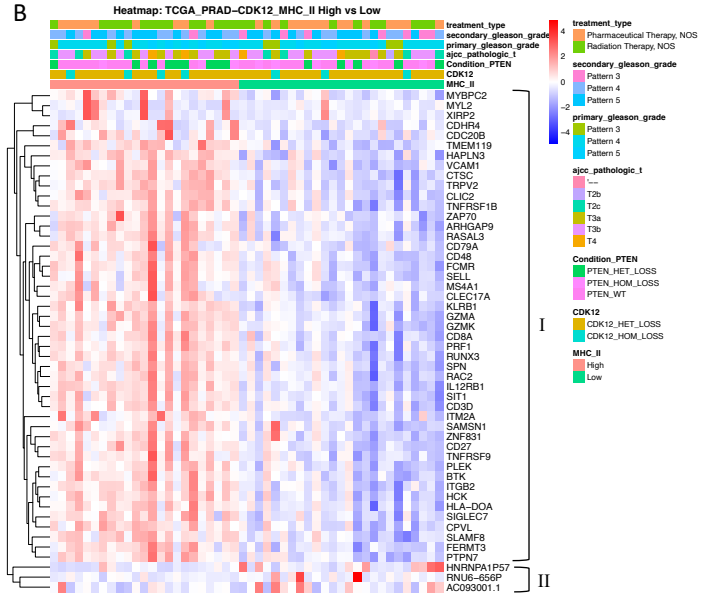
B
Heatmap: TCGA_PRAD–CDK12_MHC_II High vs Low
treatment_type
secondary_gleason_grade
primary_gleason_grade
ajcc_pathologic_t
Condition_PTEN
CDK12
MHC_II
MYBPC2
MYL2
XIRP2
CDHR4
CDC20B
TMEM119
HAPLN3
VCAM1
CTSC
TRPV2
CLIC2
TNFRSF1B
ZAP70
ARHGAP9
RASAL3
CD79A
CD48
FCMR
SELL
MS4A1
CLEC17A
KLRB1
GZMA
GZMK
CD8A
PRF1
RUNX3
SPN
RAC2
IL12RB1
SIT1
CD3D
ITM2A
SAMSN1
ZNF831
CD27
TNFRSF9
PLEK
BTK
ITGB2
HCK
HLA–DOA
SIGLEC7
CPVL
SLAMF8
FERMT3
PTPN7
HNRNPA1P57
RNU6–656P
AC093001.1
I
II
treatment_type
Pharmaceutical Therapy, NOS
Radiation Therapy, NOS
secondary_gleason_grade
Pattern 3
Pattern 4
Pattern 5
primary_gleason_grade
Pattern 3
Pattern 4
Pattern 5
ajcc_pathologic_t
'–––
T2b
T2c
T3a
T3b
T4
Condition_PTEN
PTEN_HET_LOSS
PTEN_HOM_LOSS
PTEN_WT
CDK12
CDK12_HET_LOSS
CDK12_HOM_LOSS
MHC_II
High
Low

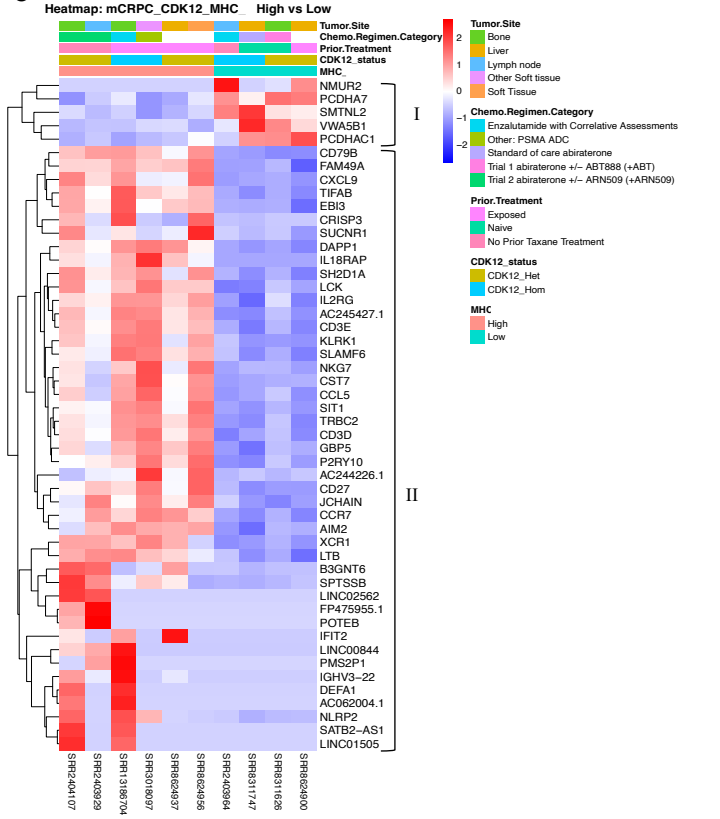
C
Heatmap: mCRPC_CDK12_MHC_ High vs Low
Tumor.Site
Chemo.Regimen.Category
Prior.Treatment
CDK12_status
MHC_
NMUR2
PCDHA7
SMTNL2
VWA5B1
PCDHAC1
CD79B
FAM49A
CXCL9
TIFAB
EBI3
CRISP3
SUCNR1
DAPP1
IL18RAP
SH2D1A
LCK
IL2RG
AC245427.1
CD3E
KLRK1
SLAMF6
NKG7
CST7
CCL5
SIT1
TRBC2
CD3D
GBP5
P2RY10
AC244226.1
CD27
JCHAIN
CCR7
AIM2
XCR1
LTB
B3GNT6
SPTSSB
LINC02562
FP475955.1
POTEB
IFIT2
LINC00844
PMS2P1
IGHV3–22
DEFA1
AC062004.1
NLRP2
SATB2–AS1
LINC01505
SRR2404107
SRR2403929
SRR13186704
SRR3016097
SRR8624937
SRR8624956
SRR2403964
SRR8311747
SRR8311626
SRR8624900
I
II
Tumor.Site
Bone
Liver
Lymph node
Other Soft tissue
Soft Tissue
Chemo.Regimen.Category
Enzalutamide with Correlative Assessments
Other: PSMA ADC
Standard of care abiraterone
Trial 1 abiraterone +/– ABT888 (+ABT)
Trial 2 abiraterone +/– ARN509 (+ARN509)
Prior.Treatment
Exposed
Naive
No Prior Taxane Treatment
CDK12_status
CDK12_Het
CDK12_Hom
MHC
High
Low

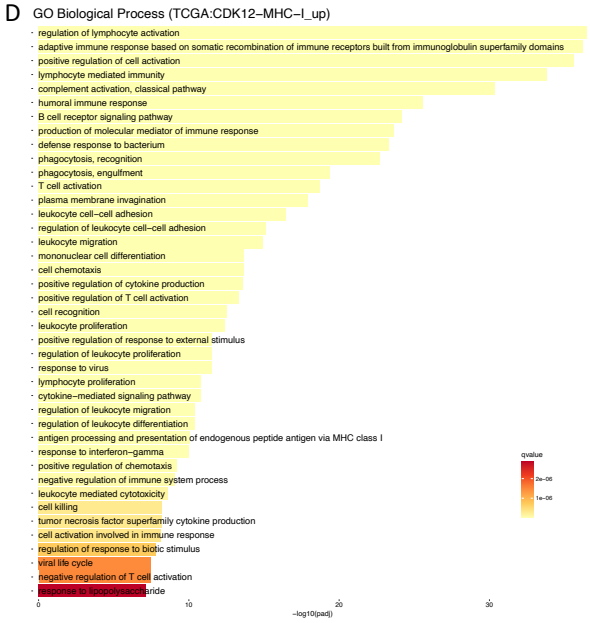
D
GO Biological Process (TCGA:CDK12–MHC–I_up)
regulation of lymphocyte activation
adaptive immune response based on somatic recombination of immune receptors built from immunoglobulin superfamily domains
positive regulation of cell activation
lymphocyte mediated immunity
complement activation, classical pathway
humoral immune response
B cell receptor signaling pathway
production of molecular mediator of immune response
defense response to bacterium
phagocytosis, recognition
phagocytosis, engulfment
T cell activation
plasma membrane invagination
leukocyte cell–cell adhesion
regulation of leukocyte cell–cell adhesion
leukocyte migration
mononuclear cell differentiation
cell chemotaxis
positive regulation of cytokine production
positive regulation of T cell activation
cell recognition
leukocyte proliferation
positive regulation of response to external stimulus
regulation of leukocyte proliferation
response to virus
lymphocyte proliferation
cytokine–mediated signaling pathway
regulation of leukocyte migration
regulation of leukocyte differentiation
antigen processing and presentation of endogenous peptide antigen via MHC class I
response to interferon–gamma
positive regulation of chemotaxis
negative regulation of immune system process
leukocyte mediated cytotoxicity
cell killing
tumor necrosis factor superfamily cytokine production
cell activation involved in immune response
regulation of response to biotic stimulus
viral life cycle
negative regulation of T cell activation
response to lipopolysaccharide
qvalue
2e–06
1e–06
0
10
20
30
−log10(padj)

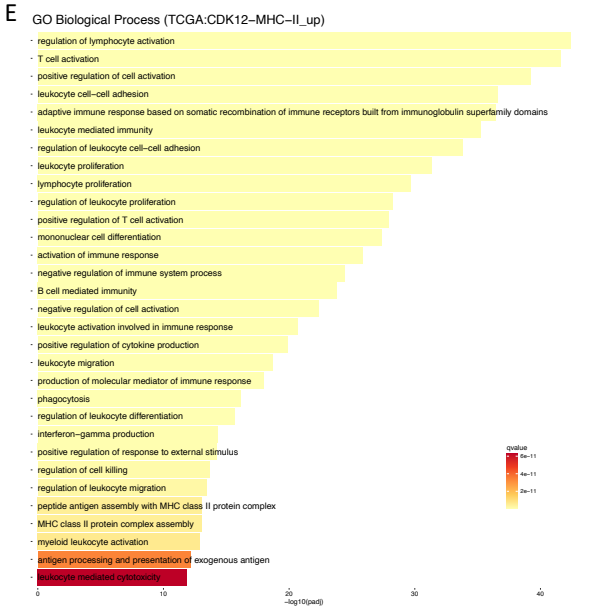
E
GO Biological Process (TCGA:CDK12–MHC–II_up)
regulation of lymphocyte activation
T cell activation
positive regulation of cell activation
leukocyte cell–cell adhesion
adaptive immune response based on somatic recombination of immune receptors built from immunoglobulin superfamily domains
leukocyte mediated immunity
regulation of leukocyte cell–cell adhesion
leukocyte proliferation
lymphocyte proliferation
regulation of leukocyte proliferation
positive regulation of T cell activation
mononuclear cell differentiation
activation of immune response
negative regulation of immune system process
B cell mediated immunity
negative regulation of cell activation
leukocyte activation involved in immune response
positive regulation of cytokine production
leukocyte migration
production of molecular mediator of immune response
phagocytosis
regulation of leukocyte differentiation
interferon–gamma production
positive regulation of response to external stimulus
regulation of cell killing
regulation of leukocyte migration
peptide antigen assembly with MHC class II protein complex
MHC class II protein complex assembly
myeloid leukocyte activation
antigen processing and presentation of exogenous antigen
leukocyte mediated cytotoxicity
qvalue
6e–11
4e–11
2e–11
0
10
20
30
40
−log10(padj)

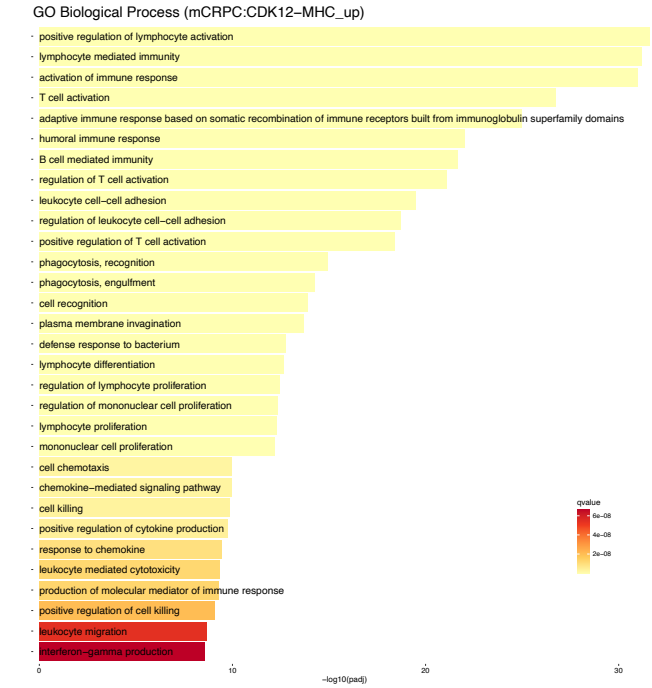
F
GO Biological Process (mCRPC:CDK12–MHC_up)
positive regulation of lymphocyte activation
lymphocyte mediated immunity
activation of immune response
T cell activation
adaptive immune response based on somatic recombination of immune receptors built from immunoglobulin superfamily domains
humoral immune response
B cell mediated immunity
regulation of T cell activation
leukocyte cell–cell adhesion
regulation of leukocyte cell–cell adhesion
positive regulation of T cell activation
phagocytosis, recognition
phagocytosis, engulfment
cell recognition
plasma membrane invagination
defense response to bacterium
lymphocyte differentiation
regulation of lymphocyte proliferation
regulation of mononuclear cell proliferation
lymphocyte proliferation
mononuclear cell proliferation
cell chemotaxis
chemokine–mediated signaling pathway
cell killing
positive regulation of cytokine production
response to chemokine
leukocyte mediated cytotoxicity
production of molecular mediator of immune response
positive regulation of cell killing
leukocyte migration
interferon–gamma production
qvalue
6e–08
4e–08
2e–08
0
10
20
30
−log10(padj)

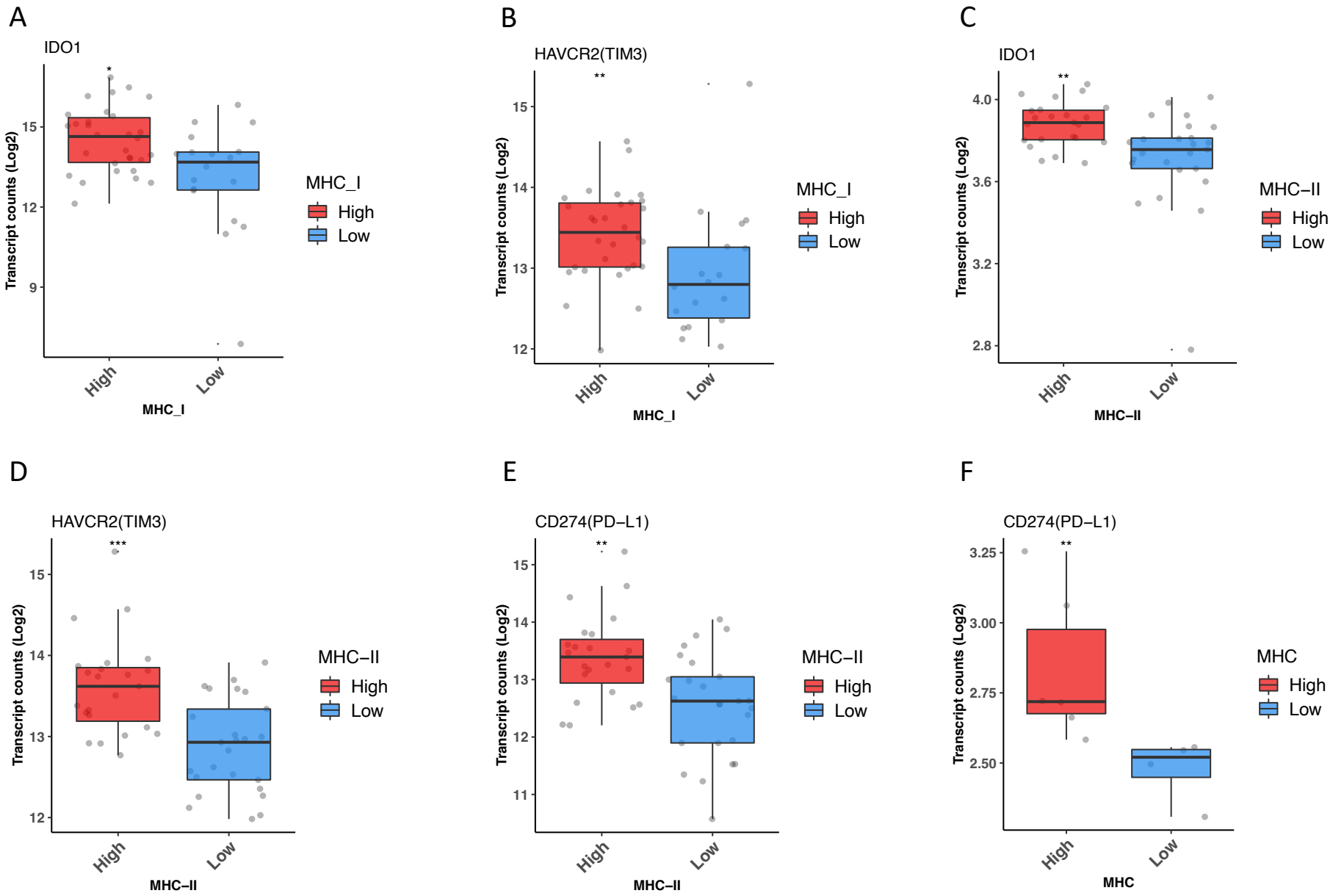
A
IDO1
Transcript counts (Log2)
MHC_I
High
Low
B
HAVCR2(TIM3)
Transcript counts (Log2)
MHC_I
High
Low
C
IDO1
Transcript counts (Log2)
MHC–II
High
Low
D
HAVCR2(TIM3)
Transcript counts (Log2)
MHC–II
High
Low
E
CD274(PD–L1)
Transcript counts (Log2)
MHC–II
High
Low
F
CD274(PD–L1)
Transcript counts (Log2)
MHC
High
Low

A)

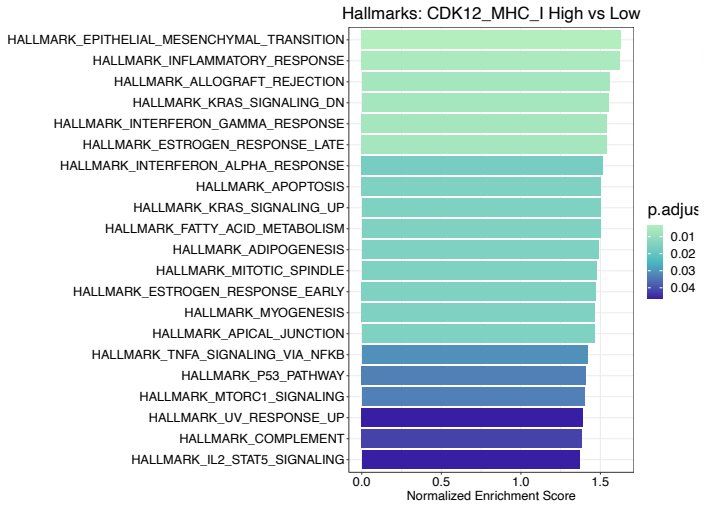
Hallmarks: CDK12_MHC_I High vs Low
HALLMARK_EPITHELIAL_MESENCHYMAL_TRANSITION
HALLMARK_INFLAMMATORY_RESPONSE
HALLMARK_ALLOGRAFT_REJECTION
HALLMARK_KRAS_SIGNALING_DN
HALLMARK_INTERFERON_GAMMA_RESPONSE
HALLMARK_ESTROGEN_RESPONSE_LATE
HALLMARK_INTERFERON_ALPHA_RESPONSE
HALLMARK_APOPTOSIS
HALLMARK_KRAS_SIGNALING_UP
HALLMARK_FATTY_ACID_METABOLISM
HALLMARK_ADIPOGENESIS
HALLMARK_MITOTIC_SPINDLE
HALLMARK_ESTROGEN_RESPONSE_EARLY
HALLMARK_MYOGENESIS
HALLMARK_APICAL_JUNCTION
HALLMARK_TNFA_SIGNALING_VIA_NFKB
HALLMARK_P53_PATHWAY
HALLMARK_MTORC1_SIGNALING
HALLMARK_UV_RESPONSE_UP
HALLMARK_COMPLEMENT
HALLMARK_IL2_STAT5_SIGNALING
0.0
0.5
1.0
1.5
Normalized Enrichment Score
p.adjus
0.01
0.02
0.03
0.04

B)

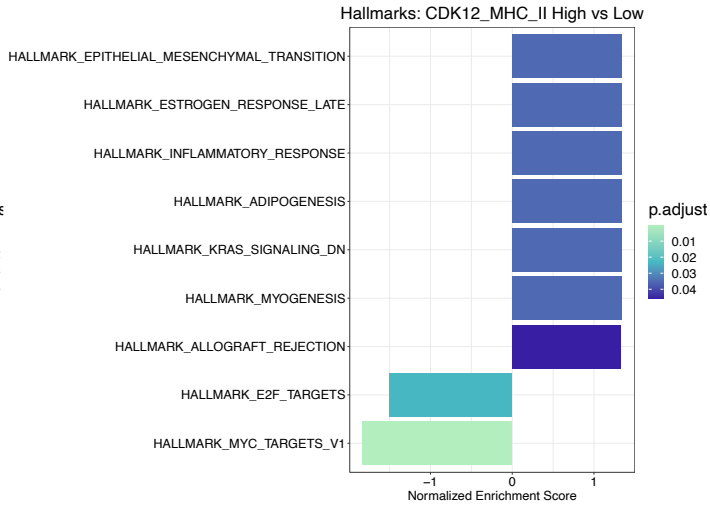
Hallmarks: CDK12_MHC_II High vs Low
HALLMARK_EPITHELIAL_MESENCHYMAL_TRANSITION
HALLMARK_ESTROGEN_RESPONSE_LATE
HALLMARK_INFLAMMATORY_RESPONSE
HALLMARK_ADIPOGENESIS
HALLMARK_KRAS_SIGNALING_DN
HALLMARK_MYOGENESIS
HALLMARK_ALLOGRAFT_REJECTION
HALLMARK_E2F_TARGETS
HALLMARK_MYC_TARGETS_V1
−1
0
1
Normalized Enrichment Score
p.adjust
0.01
0.02
0.03
0.04

C)

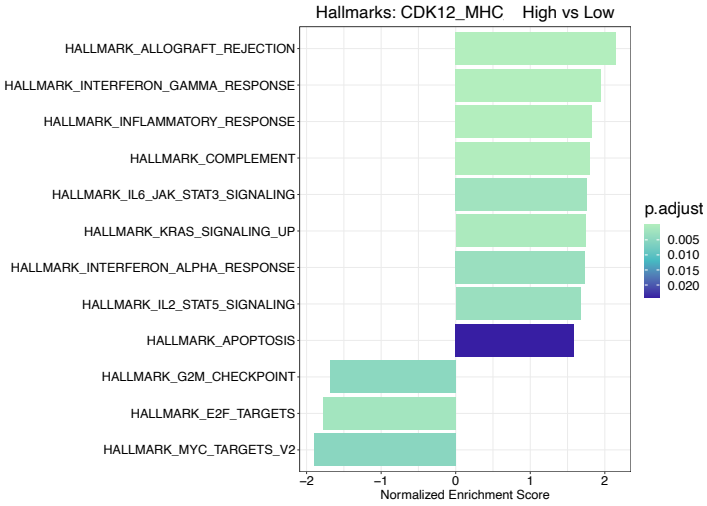
Hallmarks: CDK12_MHC High vs Low
HALLMARK_ALLOGRAFT_REJECTION
HALLMARK_INTERFERON_GAMMA_RESPONSE
HALLMARK_INFLAMMATORY_RESPONSE
HALLMARK_COMPLEMENT
HALLMARK_IL6_JAK_STAT3_SIGNALING
HALLMARK_KRAS_SIGNALING_UP
HALLMARK_INTERFERON_ALPHA_RESPONSE
HALLMARK_IL2_STAT5_SIGNALING
HALLMARK_APOPTOSIS
HALLMARK_G2M_CHECKPOINT
HALLMARK_E2F_TARGETS
HALLMARK_MYC_TARGETS_V2
−2
−1
0
1
2
Normalized Enrichment Score
p.adjust
0.005
0.010
0.015
0.020

D)

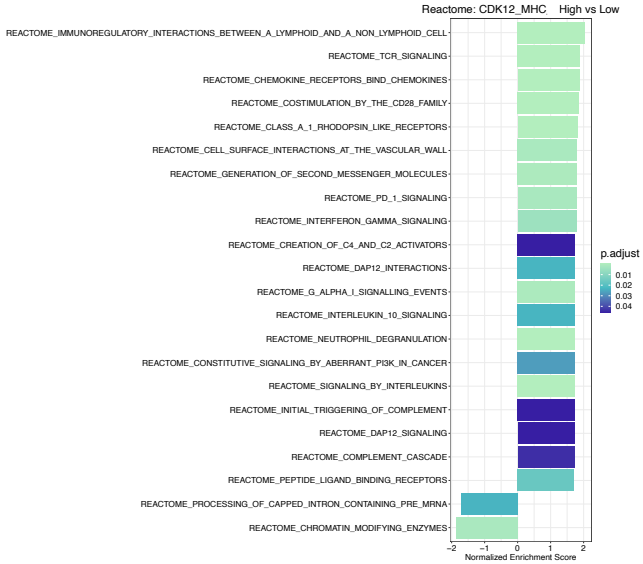
Reactome: CDK12_MHC High vs Low
REACTOME_IMMUNOREGULATORY_INTERACTIONS_BETWEEN_A_LYMPHOID_AND_A_NON_LYMPHOID_CELL
REACTOME_TCR_SIGNALING
REACTOME_CHEMOKINE_RECEPTORS_BIND_CHEMOKINES
REACTOME_COSTIMULATION_BY_THE_CD28_FAMILY
REACTOME_CLASS_A_1_RHODOPSIN_LIKE_RECEPTORS
REACTOME_CELL_SURFACE_INTERACTIONS_AT_THE_VASCULAR_WALL
REACTOME_GENERATION_OF_SECOND_MESSENGER_MOLECULES
REACTOME_PD_1_SIGNALING
REACTOME_INTERFERON_GAMMA_SIGNALING
REACTOME_CREATION_OF_C4_AND_C2_ACTIVATORS
REACTOME_DAP12_INTERACTIONS
REACTOME_G_ALPHA_I_SIGNALLING_EVENTS
REACTOME_INTERLEUKIN_10_SIGNALING
REACTOME_NEUTROPHIL_DEGRANULATION
REACTOME_CONSTITUTIVE_SIGNALING_BY_ABERRANT_PI3K_IN_CANCER
REACTOME_SIGNALING_BY_INTERLEUKINS
REACTOME_INITIAL_TRIGGERING_OF_COMPLEMENT
REACTOME_DAP12_SIGNALING
REACTOME_COMPLEMENT_CASCADE
REACTOME_PEPTIDE_LIGAND_BINDING_RECEPTORS
REACTOME_PROCESSING_OF_CAPPED_INTRON_CONTAINING_PRE_MRNA
REACTOME_CHROMATIN_MODIFYING_ENZYMES
−2
−1
0
1
2
Normalized Enrichment Score
p.adjust
0.01
0.02
0.03
0.04

A)

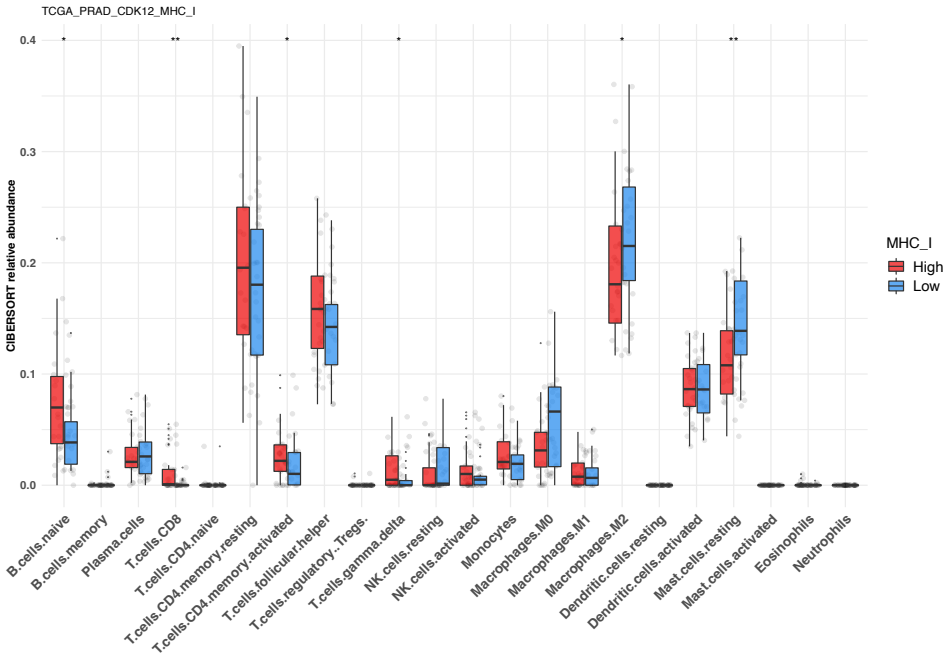
TCGA_PRAD_CDK12_MHC_I
CIBERSORT relative abundance
0.0
0.1
0.2
0.3
0.4
B.cells.naive
B.cells.memory
Plasma.cells
T.cells.CD8
T.cells.CD4.naive
T.cells.CD4.memory.resting
T.cells.CD4.memory.activated
T.cells.follicular.helper
T.cells.regulatory..Tregs.
T.cells.gamma.delta
NK.cells.resting
NK.cells.activated
Monocytes
Macrophages.M0
Macrophages.M1
Macrophages.M2
Dendritic.cells.resting
Dendritic.cells.activated
Mast.cells.resting
Mast.cells.activated
Eosinophils
Neutrophils
MHC_I
High
Low

B)

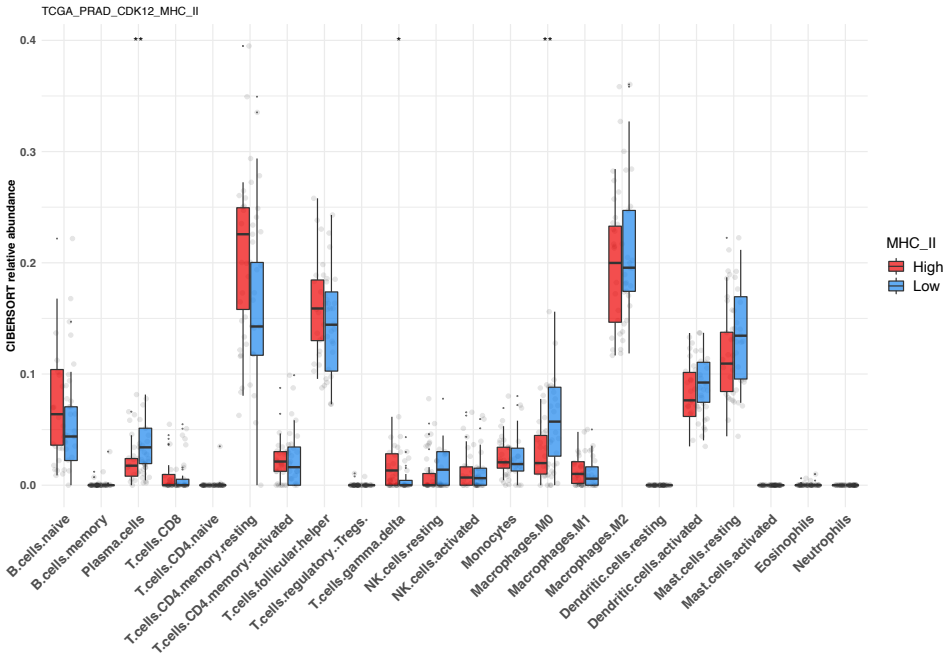
TCGA_PRAD_CDK12_MHC_II
CIBERSORT relative abundance
0.0
0.1
0.2
0.3
0.4
B.cells.naive
B.cells.memory
Plasma.cells
T.cells.CD8
T.cells.CD4.naive
T.cells.CD4.memory.resting
T.cells.CD4.memory.activated
T.cells.follicular.helper
T.cells.regulatory..Tregs.
T.cells.gamma.delta
NK.cells.resting
NK.cells.activated
Monocytes
Macrophages.M0
Macrophages.M1
Macrophages.M2
Dendritic.cells.resting
Dendritic.cells.activated
Mast.cells.resting
Mast.cells.activated
Eosinophils
Neutrophils
MHC_II
High
Low

C)

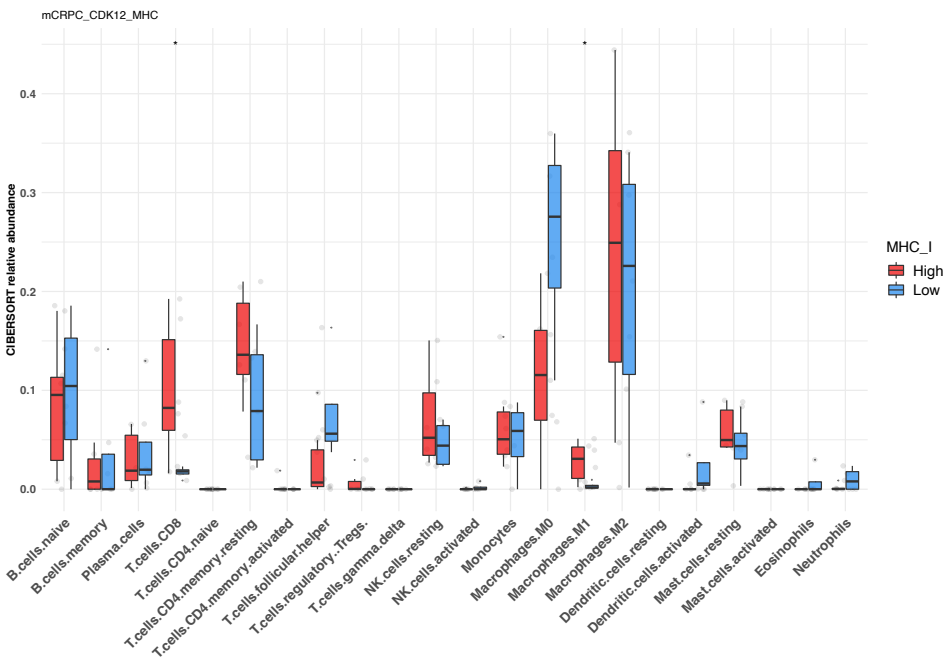
mCRPC_CDK12_MHC
CIBERSORT relative abundance
0.0
0.1
0.2
0.3
0.4
B.cells.naive
B.cells.memory
Plasma.cells
T.cells.CD8
T.cells.CD4.naive
T.cells.CD4.memory.resting
T.cells.CD4.memory.activated
T.cells.follicular.helper
T.cells.regulatory..Tregs.
T.cells.gamma.delta
NK.cells.resting
NK.cells.activated
Monocytes
Macrophages.M0
Macrophages.M1
Macrophages.M2
Dendritic.cells.resting
Dendritic.cells.activated
Mast.cells.resting
Mast.cells.activated
Eosinophils
Neutrophils
MHC_I
High
Low